https://dx.doi.org/10.22161/ijaers/3.11.29 *ISSN: 2349-6495(P) | 2456-1908(O)*

Electrochemical Behavior of Cu-Al-Ni Alloy in Simulated Body Fluids

Rabab M. El-Sherif

Chemistry Department, Faculty of Science, Cairo University, Gamaa Street, 12613 Giza, Egypt.

Abstract— *The electrochemical comparative studies between, Cu-Al-Ni alloy as a non-precious casting alloy and a pure Ti as a common biomaterial were investigated in simulated body fluid (SBF). The aim of the work was to evaluate the corrosion resistivity of these alloys in the simulated body fluids, using electrochemical impedance spectroscopy (EIS) and potentiodynamic polarization measurements. The surface morphology of the alloys was examined via the scanning electron microscopy. This comparison was focused on the effect of the solution chemistry and immersion time on the passivity of the alloys. The influence of albumin, as a model protein, and a fluoride ion with its simulated dose in a human body, on both biomaterials was investigated. The Albumin has enhanced the corrosion resistance of both samples. On the contrary, fluoride ion increased their corrosion rate in all the tested solutions. The electrochemical behavior of Ti has shown a higher transfer resistance and a lower capacitance compared with the copper alloy. However, the resistivity of both materials increased with immersion time in the different solutions.*

Keywords— Biomaterials, Corrosion, Cu-Al-Ni alloy, impedance, Polarization, SEM.

I. INTRODUCTION

Titanium and its alloys have been widely used in the last decades as biocompatible materials for dental implants, orthopedic implants and medical devices [1-5]. This is due to a passive film formation on their surface, consisting mainly of amorphous titanium dioxide (TiO_2), which is responsible for their biocompatibility and corrosion resistance in several media, including the human body environment [6, 7]. A contact between the metallic implant and the living tissues takes place through the oxide layer on the implant surface during the osseointegration process [8].

Nowadays in the prosthetic dentistry field “non precious” alloys (Ni and Co based) substitutes the much more expensive precious metal alloys (Pt, Au, Pd and Ti) [8]. Copper-based alloys have been used in many practical applications because of their good corrosion resistance, and excellent physical properties [9-11]. The addition of aluminum to Cu-based alloys increases its corrosion resistance while the presence of nickel is essential in the passivation of Cu-Ni alloys. The passivation of the alloy is attributed to the greater affinity of aluminum toward oxygen than copper and a considerable stability of Al_2O_3 than Cu_2O in neutral solutions [12, 13]. Different corrosion studies of aluminum bronze in artificial saliva, acidic and saline solutions showed that 0.9% saline solution is more corrosive than artificial saliva [14]. Also, ‘passivation’ was observed in artificial saliva and Na_2S solutions, but not in citric acid or KCl solutions [15]. One of the main challenging issues that faces the casting non-precious alloys is the release of elements into the body over the short-term (days) and long term (months) during corrosion[16-22]. For some metals and alloys, elemental release during corrosion can be affected significantly by biological environments in vitro and in vivo, and specifically in the presence of proteins [23]. In vitro, proteins show an increase of the corrosion rate of some alloys and pure metals such as stainless steel, copper, nickel and titanium [24, 25]. However, few studies have considered the effects of proteins on the elemental release from dental casting alloys. Liu [26] has found that the corrosion resistance in simulated body fluid (SBF) + 1 g/L albumin is almost twice that in SBF alone. The electrochemical behavior of WE43 alloy in SBF in the absence and presence of 40 g/L albumin was investigated by Retting [27, 28].

In the present work, it is aimed to assess the influence of the simulated body fluid in the presence of albumin, as a model protein, and a fluoride ion with its simulated dose in a human body on the passivation and dissolution behavior of Cu-Al-Ni and Ti metal at about 37 ˚C. The study is furthermore aimed to improve knowledge of the nature of the formed passive films in these systems by comparing the behavior of Cu-Al-Ni as a non-precious low cost alloy with titanium, using potentiodynamic, electrochemical impedance spectroscopy techniques and scanning electron microscopy.

II. EXPERIMENTAL

2.1 Materials and solutions

Two samples of pure titanium (99.99%) and Cu-Al-Ni alloy with composition of wt. %; 9.71 Al, 5.03 Ni, 3.05 Fe, 1.06 Mn, 0.02 Si, 0.02 Sn, and 81.11 Cu were used in this study. The electrodes were supplied in the form of

https://dx.doi.org/10.22161/ijaers/3.11.29 *ISSN: 2349-6495(P) | 2456-1908(O)*

cylindrical rods from Johnson and Malthey (England) with exposed surface area of 0.4 and 0.5cm^2 for titanium and Cu-Al-Ni alloy, respectively. The electrodes surfaces were successively polished with finer grades of emery paper (600–1200 grade) to obtain a mirror-like image. A conventional three-electrode cell was used with a saturated calomel reference electrode (SCE) (E_{SCE} = 0.242 V vs. NHE) and a rectangular platinum sheet as counter electrode. The experiments were carried out using three simulated body solutions: naturally aerated aqueous simulated body fluid (SBF) (NaCl 8.74 g/l, $NaHCO_3$ 0.35 g/l, Na_2HPO_4 0.06 g/l, NaH_2PO_4 0.06 g/l, PH 7.4), SBF with 0.5 g/l albumin and SBF with 4.4 mg/l KF (simulated dose in the human body) in order to analyze the influence of fluoride ion and albumin on the electrochemical behavior of the biomaterials .The solutions were prepared from Analytical grade reagents and triply distilled water. Temperature of the solutions was kept out ± 37 ^oC and pH 7.4 (human body conditions).

2.2 Electrochemical Techniques

All the electrochemical measurements, including open-circuit potential E_{oc}, potentiodynamic and electrochemical impedance spectroscopy (EIS) were carried out using the electrochemical workstation IM6e Zahner-electrik GmbH (Mebtechnik, Kronach, Germany) provided with Thales software. Open-circuit potential measurements, E_{oc}, for each material were measured on a freshly polished sample, in naturally aerated aqueous solutions without stirring, for 24 h. Potentiodynamic polarization tests were performed after one hour of immersion in the tested solutions. The cathodic and anodic polarization scans were carried out at 2 mVs^{-1} scan rate vs. SCE. Electrochemical impedance spectroscopy (EIS) measurements were studied at the open-circuit potential. The impedance spectra were acquired in the frequency range from 0.1 Hz up to 10 kHz with a perturbation signal of 10 mV. EIS plots were obtained after the specimens were immersed in the test solution for different time immersion up to 24 h. SEM micrographs were conducted using a JEOL JXA-840 A electron probe micro analyzer. The experiments were always carried out at 37 ^oC, unless otherwise stated.

III. RESULTS AND DISCUSSION

3.1 Open-circuit potential analyses

The open-circuit potential (E_{oc}) of pure Ti and Cu–Al-Ni alloy was followed over a period of 24 h in three media, simulated body fluid (SBF), SBF+ Albumin and SBF+ KF. The results were presented in Figs. 1, 2. E_{oc} changed towards more positive potentials during the first hour of electrode immersion in different solutions. After that, E_{oc} changed slowly until it reached a quasi-stationary state after three hours. No significant change occurred after that. This indicated that a spontaneously passive film is formed with time on both Cu-Al-Ni and pure Ti surfaces. The addition of fluoride ion shifted the potential towards more negative values in both samples. This is because; fluoride addition to the solution made Ti potential more active and enhanced its corrosion. In other words, fluoride ion affected the electrochemical activity of Ti [29-31].

On the other hand, adding albumin to the SBF solution shifted the potential towards more positive values for both samples (Cf. Figs. 1, 2). It is known that a layer of adsorbed proteins is formed immediately on the dental implant surface after being into the oral cavity, which enhances the biocompatibility of the implant. Therefore, the naturally contained proteins in the human saliva may play an important role in the corrosion resistance of dental implant materials, e.g. Ti and Ti-based alloys. The presence of protein (bovine albumin) in phosphate buffered saline (PBS) increased the corrosion resistance of Ti–6Al–4V, but decreased that of Ti–13Nb–13Zr and Ti–6Al–7Nb [32, 33]. Obviously, the presence of proteins, albumin would affect the corrosion resistance of titanium alloys.

3.2 Potentiodynamic polarization

Figs. 3, 4 showed the potentiodynamic polarization curves of Ti and Cu-Al-Ni alloy in the three solutions: SBF, SBF+ KF and SBF+ Albumin respectively. The polarization curves of Cu-Al-Ni revealed an active-to-passive transition behavior in all the tested solutions, whereas Ti showed a totally passive behavior. The passivation and corrosion behavior of the Cu-Al-Ni alloy could be explained on the basis of the data reported on Cu and cast nickel-aluminum bronze [34-37]. The copper dissolution reaction represented the major anodic process. Whereas, the cathodic reaction was mainly due to oxygen reduction, as seen in the following equation:

$$O_2 + 2H_2O + 4e^- \rightarrow 4OH^- \quad [E^o = 0.401 \text{ V vs. SHE}] \quad (1)$$

The corrosion resistance of the Cu-Al-Ni alloy was mainly due to the duplex nature of the protective layer containing both Cu_2O and Al_2O_3 [38].

On adding albumin to the solution, the cathodic current density was significantly decreased. All the corrosion parameters were estimated and presented in Tables 1, 2. Since the albumin isoelectric point is known to be 4.9 [39], so it was expected that albumin is negatively charged at the pH of the tested solutions (pH7.4). As the alloy surface was polarized in the positive direction where electron depletion was created, the adsorption of negatively charged species of albumin on the electrode surface was detected.

On the contrary, addition of fluoride ion increased the corrosion current density significantly and shifted the

https://dx.doi.org/10.22161/ijaers/3.11.29 *ISSN: 2349-6495(P) | 2456-1908(O)*

corrosion potential to more negative direction (cf. Tables 1, 2). The increase of the current density in the presence of fluoride ion could be explained by the dissolution of the protective oxide film. The structure of oxide layer may be affected by the fluoride ion and become more porous, which leads to a decrease in its resistance. Generally, the effect of fluoride ion depends on its concentration and the solution pH [40].

3.3 Electrochemical impedance spectroscopy measurements

Impedance spectra of pure Ti and Cu-Al-Ni alloy at different immersion times in SBF, SBF+ Albumin and SBF + KF solutions were represented as Bode plots, in Fig. 5 (a, b, c) and Fig. 6 (a, b, c) respectively. The presence of additional time constants in the impedance spectra at different frequency range was predicted from the phase angle, Θ. It is usually more preferable to use Bode plots format as, it presents all experimental data over the entire frequency domain [41].

After one hour of immersion, both of the tested samples exhibited low impedance values. The total impedance was considerably increased with immersion time. However, no significant change in the behavior was observed after 24 h. This trend could be due to the surface full coverage with spontaneous oxide layers [42]. The broadening of the Bode plots spectra and the increase of the phase angle with immersion time indicated a decrease in the corrosion rate of the alloys. The increase in the charge transfer resistance of the surface oxide film reflected the improvements of the corrosion resistance of the alloy with the immersion time [43]. The Bode plots in the frequency domain 0.1 Hz up to 10 kHz showed two time constants with a phase angle close to 80^o for pure Ti and 70^o for Cu-Al-Ni alloy. The relation between the frequency (log f) and the impedance (log |Z|) was observed to be a linear one with a slope near to 1. After 24 h of immersion, the phase angle of Ti remained near 80^o even at low frequencies, and 70^o for the copper alloy. This indicated a near-capacitive response for both samples. However, the alloys immersed for 24 h in SBF solution showed two time constants spectra with a bi-layered surface corresponding to an inner layer and an outer one.

The equivalent circuit shown in Fig. 7 was the best fitting for all the experimental data. Where, R_s, CPE_1 and R_1 are the solution resistance, a constant- phase element corresponding to the double layer capacitance and the charge transfer resistance, respectively. CPE_2 and R_2 assigned the electrical elements of the outer layer. The electrode impedance, Z, was expressed as follows:

$$Z = Rs + [Rct/ \{1 + (2 \pi f R_{ct} C_{dl})^{\alpha}\}] \quad (2)$$

Where α is an empirical parameter ($0 \leq \alpha \leq 1$) and f is the frequency in Hz. This formula considered the deviation from the ideal RC-behavior due to surface inhomogeneties, roughness effects, and different compositions of surface layers [44, 45]. The observed first time constant at low frequency range was due to the presence of an inhomogeneous passive film [46].

It can be noted from Tables 3-8 that the capacitance decreased, in almost all cases, with the immersion time and (α) values were close to 1, so CPE showed an almost pure capacitive behavior. The increase of the film resistance R_2 with immersion time reflected a formation of a spontaneously oxide film on both cu-alloy and Ti metal as can be seen from Fig. 8 a, b. The impedance values for Ti showed better corrosion resistance than that of Cu-Ni-Al alloy in all the studied simulated body fluids. On the other hand, the copper alloy showed a remarkably high corrosion resistance, which was essentially due to the presence of a protective layer of duplex nature, containing both Cu_2O and Al_2O_3 [38, 47-48]. The inner layer was an Al-rich barrier layer which prevents a Copper dissolution from the alloy surface. The outer layer was a porous Cu-rich consisting mainly of Cu_2O passive film [38, 49]. This result was confirmed by EDX [50], where the surface showed a higher concentration of Cu and also a lower concentration of Ni due to Ni diffusion in the inner barrier layer. Al was involved in the compact inner layer and its concentration on the surface is slightly lower than the bulk. The duplex barrier layer hindered the ionic transport and consequently increased the corrosion resistance [48, 51].

In both samples, the effect of time on the resistance and capacitance depended on the solution chemistry. With respect to the influence of albumin, it increased the charge transfer resistance and the outer layer resistance of titanium and copper alloy and slightly decreased the capacitance. This was mainly due to the blocking effect of the organic molecule and the adsorption effect [46]. R_2 values of Ti increased from 592.2 kΩ cm^2 in SBF solution to 1080 kΩ cm^2 in SBF + Albumin and from 168.5 kΩ cm^2 to 292 kΩ cm^2 for the copper alloy. On contrary was the effect of KF, as it decreased significantly the impedance resistance of both samples with respect to SBF solutions (cf. Tables 3, 4, 6 and 8). The presence of the fluoride ion in the solution may affect the nature of the oxide layer and change it to a porous structure that leads to a decrease in its resistance and increase in its capacitance [52- 54].

3.4. Morphology

Fig. 8 (a-h) showed the surface morphology of Cu-Ni-Al and Ti in SBF, SBF+KF and SBF + Albumin respectively. A significant improvement of the surface morphology due to the film formation was observed in the presence of albumin in both samples (Fig.8 d, h). On the other hand, a higher dissolution and roughness of the surface was assigned in the presence of KF (Fig. 8 c, g). The sample surface became denser and the flawed regions were repaired in the presence of albumin**.** This behavior

https://dx.doi.org/10.22161/ijaers/3.11.29 *ISSN: 2349-6495(P) | 2456-1908(O)*

confirmed well the polarization and impedance measurements.

IV. CONCLUSIONS

-The electrochemical behavior Cu-Ni-Al alloy and Ti metal was investigated in simulated body fluids at the human body temperature 37 ˚C.

-The remarkably high corrosion resistance of Cu-Ni-Al was essentially due to the presence of a protective layer of duplex nature containing both Cu_2O and Al_2O_3**.**

-The effect of time on the resistance and capacitance behavior of both samples depended on the solution chemistry**.**

-The influence of albumin as a model protein in the simulated body fluid enhanced the impedance performance of both materials.

-Addition of fluoride ion to the simulated body fluid increased the corrosion current density of Ti and copper alloy.

-The corrosion resistance of both alloys has been improved with the immersion time.

-The scanning electron microscopy confirmed well the electrochemical techniques results

- Cu-Ni-Al alloy could be considered as a promising non-precious casting alloy that has a considerable high corrosion resistance in simulated body fluids.

REFERENCES

[1] Z. Cai, T. Shafer, I. Watanabe, M.E. Nunn, T. Okabe, Electrochemical characterization of cast titanium alloys, Biomaterials, vol. 24, pp. 213-218, 2003.

[2] D.w. Shoesmith, J.J. Noël, Corrosion of titanium and its alloys, in Shreir's Corrosion Fourth Edition, Volume 3, Academic Press, New York, 2010, p. 2042.

[3] A.C. Vieira, A.R. Ribeiro, L.A. Rocha, J.P. Celis, Influence of pH and corrosion inhibitors on the tribocorrosion of titanium in artificial saliva, Wear, vol. 261, pp. 994–1001, 2006.

[4] A. Abdal-Hay, A.S. Hamdy, K.A. Khalil, J.H. Lim, A novel simple one-step air jet spinning approach for deposition of poly(vinyl acetate)/hydroxyapatite composite nanofibers on Ti implants, Mater. Sci. Eng. C. 49 pp. 681–690, 2015.

[5] N. Horasawa, T. Yamashita, S. Uehara, N. Udagawa, High-performance scaffolds on titanium surfaces: Osteoblast differentiation and mineralization promoted by a globular fibrinogen layer through cell-autonomous BMP signaling, Mater. Sci. Eng. C. 46 pp. 86–96, 2015.

[6] S. Tamilselvi, V. Raman, N. Rajendran, Corrosion behavior of Ti– 6Al–7Nb and Ti–6Al–4V ELI alloys in the simulated body fluid solution by electrochemical impedance spectroscopy, Electrochim. Acta, vol. 52, pp. 839-846, 2006.

[7] M. Geetha, U. Kamachi Mudali, A.K. Gogia, R. Asokamani, Baldev Raj, Influence of microstructure and alloying elements on corrosion behavior of Ti-13Nb-13Zr alloy, Corros. Sci. vol. 46, pp. 877-892, 2004.

[8] F. Toumelin-Chemia, F. Rouelle, G. Burdairon, Corrosive properties of fluoride-containing odontologic gels against titanium, J. Dentistry, vol. 24, pp. 109-115 , 1996.

[9] E.A. Ashour, B.G. Ateya, Electrochemical behavior of a copper–aluminum alloy in concentrated alkaline solutions, Electrochim. Acta, vol. 42, pp. 243-250, 1997.

[10] X.Z. Zhou, C.P. Deng, Y.C. Su, Comparative study on the electrochemical performance of the Cu–30Ni and Cu–20Zn–10Ni alloys, J. Alloys Compd. Vol.49, pp. 92-97, 2010.

[11] Lj. Alijnovi´ c, S. Gudi´ c, M. ˇSmith, Inhibition of CuNi10Fe corrosion in seawater by sodium-diethyl-dithiocarbamate: an electrochemical and analytical study, J. Appl. Electrochem. Vol. 309, pp. 973-979, 2000.

[12] M. Gojic, L. Vrsalovic, S. Kozuh, A. Kneissl, I. Anzel, S. Gudic, B. Kosec, M. Kliskic, Electrochemical and microstructural study of Cu–Al–Ni shape memory alloy, J. Alloys Compounds vol. 509, pp. 9782-9790, 2011.

[13] J.C. Scully, The Fundamentals of Corrosion, Pergamon Press, Oxford, 1990.

[14] B.I. Johansson, L.C. Lucas, J.E. Lemons, Corrosion of copper, nickel, and gold dental casting alloys: an in vitro and in vivo study, J. Biomed. Mater. Res. 23(Suppl. A3), pp. 349-361, 1989.

[15] A.C. Guastaldi, Comparative evaluation of in vitro tarnish corrosion changes of non-precious dental alloys a function of time and storage solutions. Ph.D. Thesis, S˜ao Paulo: School of Engineering, University of S˜ao Paulo; 1987.

[16] D. Brune, Metal release from dental biomaterials, Biomaterials, vol. 7, pp. 163-175, 1986.

[17] D. Brune, Mechanisms and kinetics of metal release from dental alloys, Int Endod J. vol. 21, pp. 135-142, 1988.

[18] J.C. Wataha, R.G. Craig, C.T. Hanks, The release of elements of dental casting alloys into cell-culture medium, J. Dent. Res. Vol. 70, pp. 1014, 1991.

[19] J.D. Bumgardner, L.C. Lucas, Corrosion and cell culture evaluations of nickel-chromium dental casting alloys, J. Appl. Biomater. Vol. 5, pp. 203-213,1994.

[20] R.L.W. Messer, L.C. Lucas, Cytotoxicity evaluations of ions released from nickel-chromium

https://dx.doi.org/10.22161/ijaers/3.11.29 *ISSN: 2349-6495(P) | 2456-1908(O)*

dental alloys, J. Dent. Res. Vol. 75, pp. 255,1996 Abstract No. 1902.

[21] J.G. Gerstorfer, K.H. Sauer, K. PaÈssler, Ion release for Ni-Cr-Mo and Co- Cr-Mo casting alloys, Int. J. Prosthodont. Vol. 4, pp. 152-158 , 1991.

[22] J.S. Covington, M.A. McBride, W.F. Slagle, A.L. Disney, Quantitization of nickel and beryllium leakage from base metal casting alloys, J. Prosthet. Dent. Vol. 54, pp. 127-136, 1985.

[23] S.A. Brown, L.J. Farnsworth, K. Merritt, T.D. Crowe, In vitro and in vivo metal ion release, J. Biomed. Mater. Res, vol. 22, pp. 321-328, 1988.

[24] D.D. Zabel, S.A. Brown, K. Merritt, J.H. Payer, AES (auger electron spectroscopy) of stainless steel corroded in saline, in serum and in vivo, J. Biomed. Mater. Res, vol. 22, pp. 31-44 , 1988.

[25] G.C.F. Clark, D.F. Williams, The effects of proteins on metallic corrosion, J. Biomed. Mater. Res, vol. 16, pp. 125-134, 1982.

[26] C.L. Liu, Y.C. Xin, X.B. Tian, P.L. Chu, Degradation susceptibility of surgical magnesium alloy in artificial albumin-containing biological fluid, Journal of Materials Research, 22(2007) 1806-1814.

[27] R. Rettig, S. Virtanen, Time-dependent electrochemical characterization of the corrosion of a magnesium rare-earth alloy in simulated body fluids, Journal of Biomedial Materials Research, vol. 85, pp. 167-175, 2008.

[28] R. Rettig, S. Virtanen, Composition of corrosion layers on a magnesium rare earth alloy in simulated body fluids, Journal of Biomedial Materials Research, vol. 88, pp. 359-369, 2009.

[29] B.I. Johansson, B. Bergman, Corrosion of titanium and amalgam couples: effect of fluoride, area size, surface preparation and fabrication procedures, Dent. Mater. Vol. 11, pp. 41-46, 1995.

[30] F. Di Carlo, L.F. Ronconi, G. Gambarini, M. Andreasi Bassi, M. Quaranta, The influence of fluorides on the electrochemical interaction between titanium and amalgam couples, J. Dent. Res, vol. 80, pp. 663, 2001, (abstract no. 1096)

[31] R.W. Schutz, D.E. Thomas, Corrosion of titanium and titanium alloys, Metals handbook, vol. 13, 9th ed. Metals Park, OH: American Society for Metal (ASM) International, 1987, 669-706.

[32] M.A. Khan, R.L. Williams, D.F. Williams, Conjoint corrosion and wear in Ti alloys, Biomaterials, vol. 20, pp. 765-772, 1999.

[33] M.A. Khan, R.L. Williams, D.F. Williams DF, The corrosion behavior of Ti-6Al-4V, Ti-6Al-7Nb and Ti-13Nb-13Zr in protein solutions, Biomaterials, vol. 20, pp. 631-637, 1999.

[34] G. Kear, B.D. Barker, K.R. Stokes, F.C. Walsh, Electrochemical Corrosion Behaviour of 90-10 Cu-Ni Alloy in Chloride-Based Electrolytes, J. Appl. Electrochem. Vol. 34, pp. 659-669, 2004.

[35] J.C. Scully, The Fundamentals of Corrosion, Pergamon Press, Oxford, 1990.

[36] C. Deslouis, B. Tribollet, G. Mengoli, M.M. Musiani, Electrochemical behavior of copper in neutral aerated chloride solution. I. Steady-state investigation, J. Appl. Electrochim. Vol. 18, pp. 374-383, 1988.

[37] G. Kear, B.D. Barker, F.C. Walsh, Electrochemical corrosion of unalloyed copper in chloride media-a critical review, Corros. Sci. vol. 46, pp. 109-135, 2004.

[38] J.A. Wharton, R.C. Barik, G. Kear, R.J.K. Wood, K.R. Stokes, F.C. Walsh, The corrosion of nickel–aluminum bronze in seawater, Corros. Sci. vol. 47, pp. 3336-3367, 2005.

[39] M.A. Khan, R.L. Williams, D.F. Williams, Biomaterials, vol. 20, pp. 631–637, 1999.

[40] V. Zwilling , M. Aucouturier , E. Darque-Ceretti, Anodic oxidation of titanium and TA6V alloy in chromic media. An electrochemical approach, Electrochim. Acta, vol. 45, pp. 921-929 , 1999.

[41] M. Metikos-Hukovic, A. Kwokal, J. Piljac, The influence of niobium and vanadium on passivity of titanium-based implants in physiological solution, Biomaterials vol. 24, pp. 3765-775 , 2003.

[42] S. Tamilselvi, V. Raman, N. Rajendran, Corrosion behaviour of Ti-6Al-7Nb and Ti-6Al-4V ELI alloys in the simulated body fluid solution by electrochemical impedance spectroscopy, Electrochim. Acta, vol. 52, pp. 839-846, 2006.

[43] W.A. Badawy, S.S. El-Egamy, K.M. Ismail, Comparative study of tantalum and titanium passive films by electrochemical impedance spectroscopy, Br. Corr. J. vol. 28, pp. 133-136, 1993.

[44] K. Hladky, L.M. Calow, J.L. Dawson, Corrosion Rates from Impedance Measurements: An Introduction, Br. Corr. J. vol. 15, pp. 20-25, 1980.

[45] J. Hitzig, J. Titz, K. Juettner, W.J. Lorenz, E. Schmidt, Frequency response analysis of the Ag/Ag^{+} system: a partially active electrode approach, Electrochim. Acta, vol. 29, pp. 287-296 , 1984.

[46] A. Igual-Muñoz, S. Mischler, Interactive Effects of Albumin and Phosphate Ions on the Corrosion of CoCrMo Implant Alloy, Journal of the Electrochemical Society, vol. 154, pp. C562–C570, 2007.

[47] W.A. Badawy, F.M. Al-Kharafi, A.S. El-Azab, Electrochemical behavior and corrosion inhibition of

https://dx.doi.org/10.22161/ijaers/3.11.29 *ISSN: 2349-6495(P) | 2456-1908(O)*

Al, Al-6061 and Al-Cu in neutral aqueous solutions, Corros. Sci. vol. 41, pp. 709-727, 1999.

[48] W.A. Badawy, M. El-Rabiee, N.H. Hilal, H. Nady, Effect of nickel content on the electrochemical behavior of Cu-Al-Ni alloys in chloride free neutral solutions, Electrochim. Acta, vol. 56, pp. 913-918, 2010.

[49] W.A. Badawy, M. El-Rabiee, N.H. Hilal, H. Nady, Electrochemical behavior of Mg and some Mg alloys in aqueous solutions of different pH, Electrochim. Acta, vol. 55, pp. 1880-1887, 2010.

[50] H. Nady , N.H. Helal , M.M. El-Rabiee , W.A. Badawy, The role of Ni content on the stability of Cu-Al-Ni ternary alloy in neutral chloride solutions, Materials Chemistry and Physics, vol. 134, pp. 945-950, 2012.

[51] A. Schussler, H.E. Exner, The corrosion of nickel-aluminum bronzes in seawater-I. Protective layer formation and the passivation mechanism, Corros. Sci. vol. 34, pp. 1793-1802, 1993.

[52] N. Schiff, B. Grosgogeat, M. Lissac, F. Dalard, Biomaterials, vol. 23, pp. 1995, 2002.

[53] L. Reclaru, J.-M. Meyer, Biomaterials vol. 19, pp. 85, 1998.

[54] S.B. Basame, H.S. White, J. Electrochem. Soc. Vol. 147, pp. 1376, 2000.

HIGHLIGHTS

- Cu-Ni-Al alloy could be considered as a promising non-precious casting alloy that has a considerable high corrosion resistance in simulated body fluids.
- The considerable corrosion resistance of Cu-Al-Ni is due to a protective layer of duplex nature containing both Cu_2O and Al_2O_3.
- The presence of albumin as a model protein enhanced the impedance performance of the tested materials
- The fluoride ion addition increased the corrosion current density of the tested samples.
- The corrosion resistance of the alloys increased with immersion time.

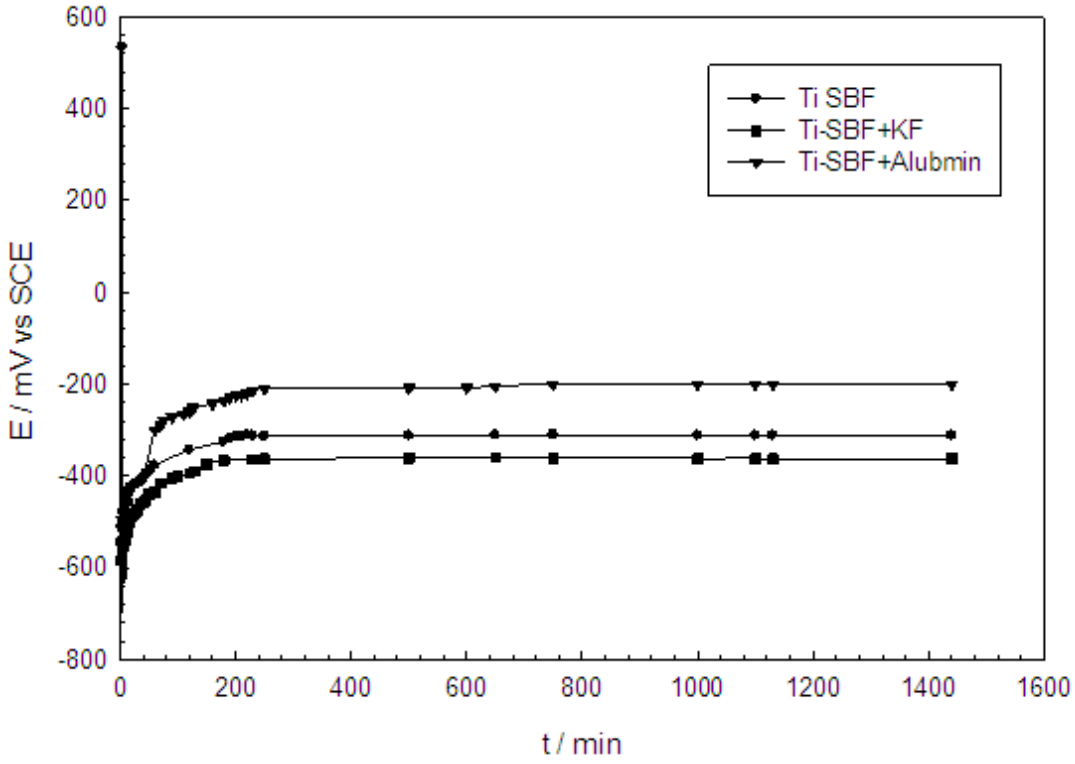

Fig. 1: Open-Circuit potential vs. time profile for pure Ti in SBF, SBF+ Albumin and SBF+ KF at 37°C.

https://dx.doi.org/10.22161/ijaers/3.11.29 *ISSN: 2349-6495(P) | 2456-1908(O)*

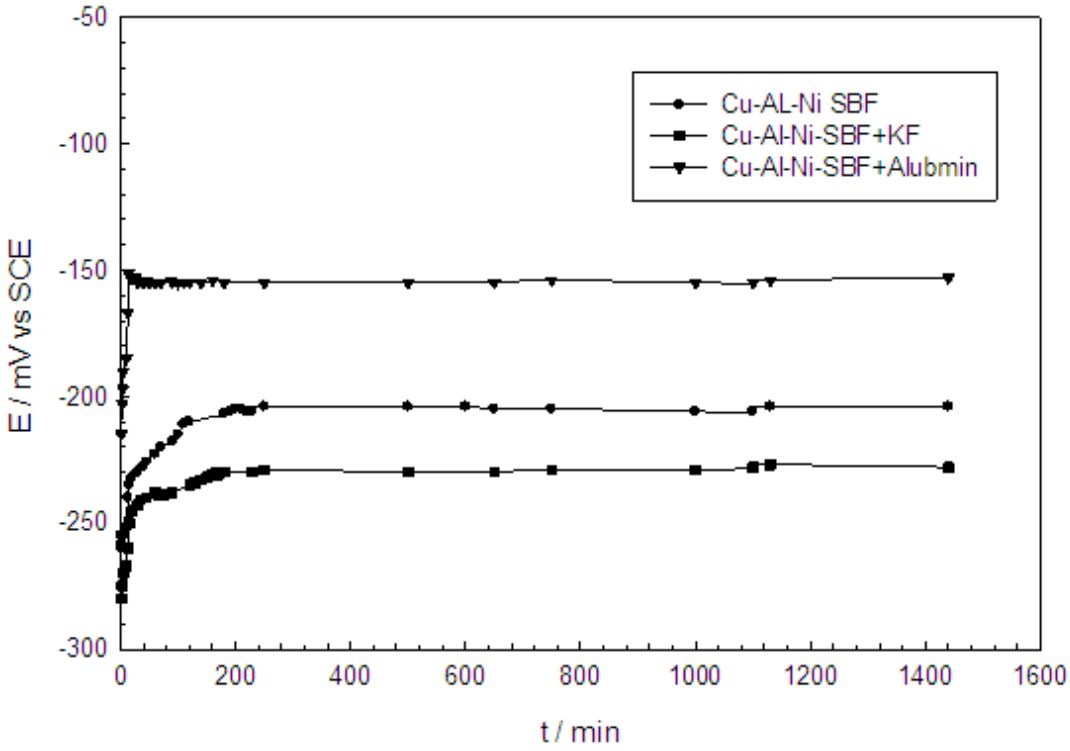

Fig. 2: Open-Circuit potential vs. time profile for Cu-Al-Ni in SBF, SBF+ Albumin and SBF+ KF at 37°C.

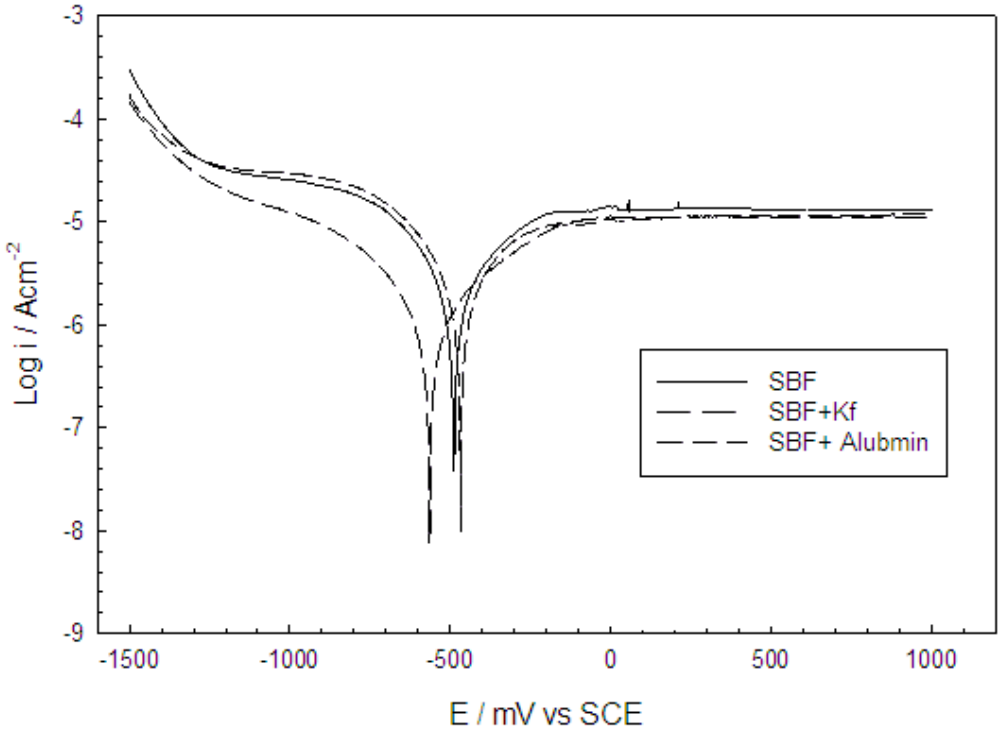

Fig. 3: Potentiodynamic polarization curves for Ti in SBF, SBF+ Albumin and SBF+ KF at 37°C.

https://dx.doi.org/10.22161/ijaers/3.11.29 *ISSN: 2349-6495(P) | 2456-1908(O)*

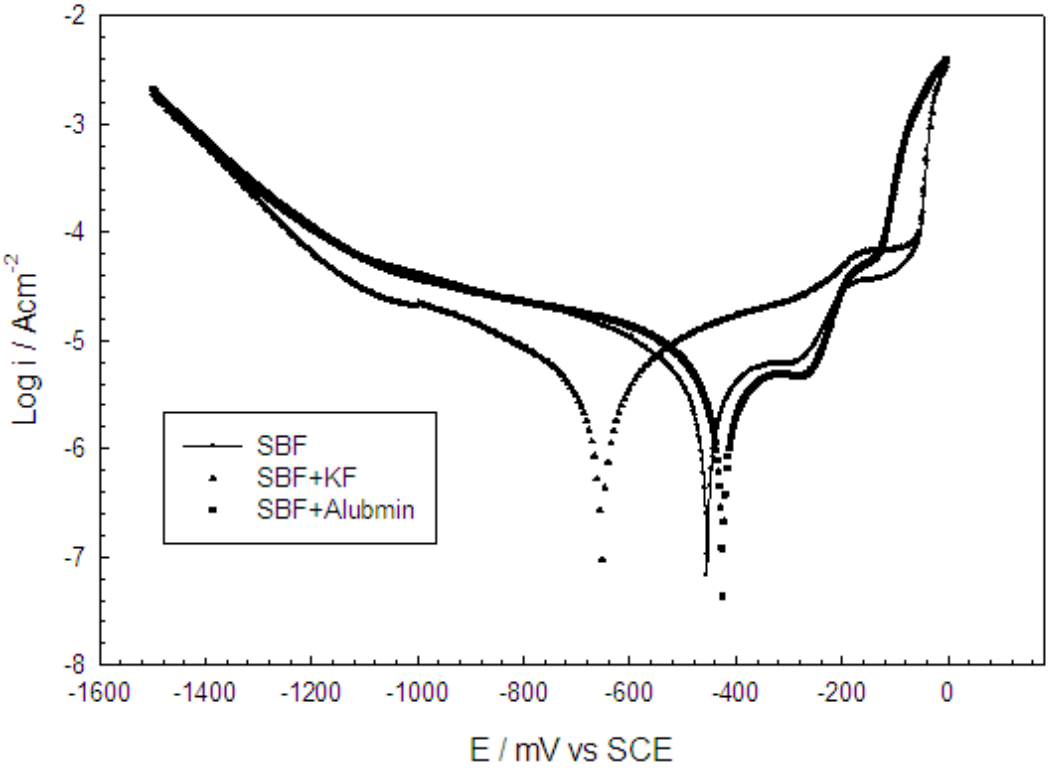

Fig. 4: Potentiodynamic polarization curves for Cu-Al-Ni in SBF, SBF+ Albumin and SBF+ KF at 37°C.

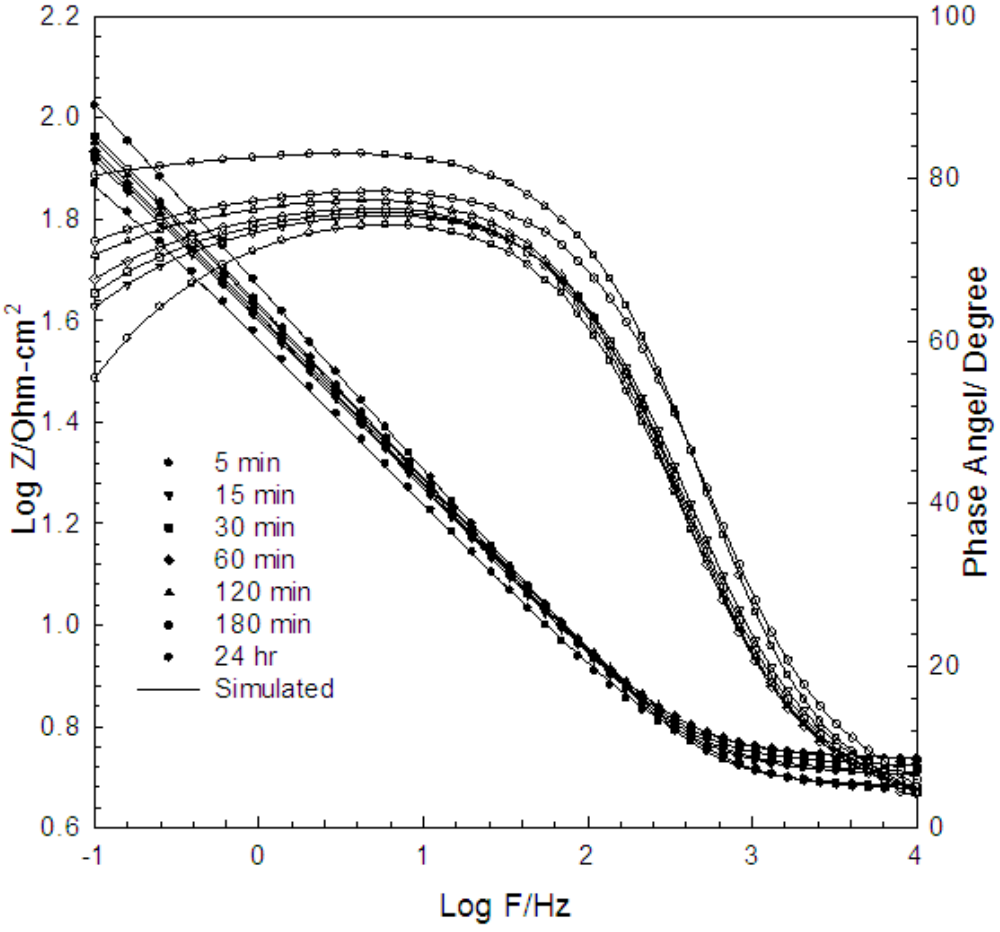

Fig. 5(a): Bode plots of Ti as a function of immersion time at 37°C in SBF solution

https://dx.doi.org/10.22161/ijaers/3.11.29 ISSN: 2349-6495(P) | 2456-1908(O)

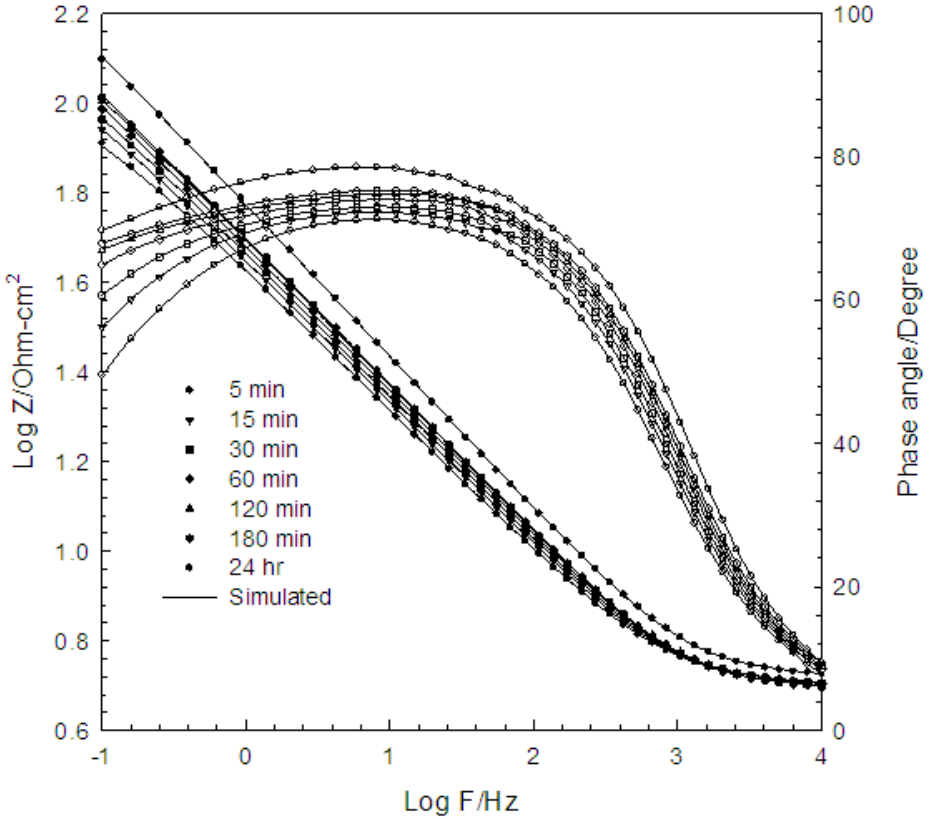

Fig. 5 (b): Bode plots of Ti as a function of immersion time at 37^{o}C in SBF +Albumin

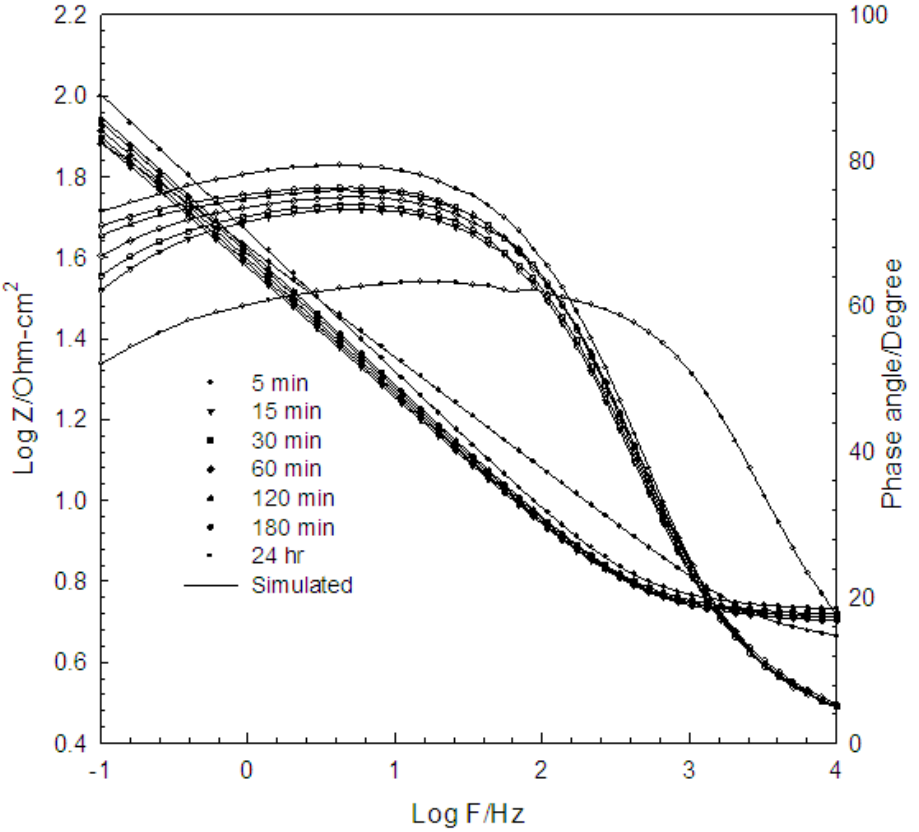

Fig. 5 (c): Bode plots of Ti as a function of immersion time at 37^{o}C in SBF +KF

https://dx.doi.org/10.22161/ijaers/3.11.29 ISSN: 2349-6495(P) | 2456-1908(O)

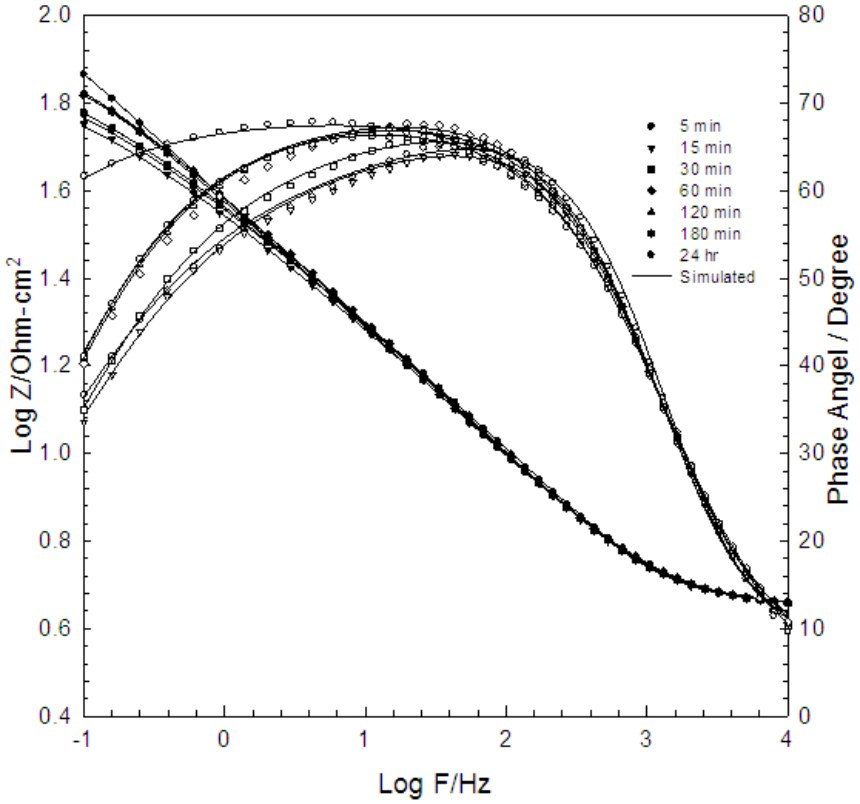

Fig. 6 (a): Bode plots of Cu-Al-Ni as a function of immersion time at 37^{o}C in SBF solution

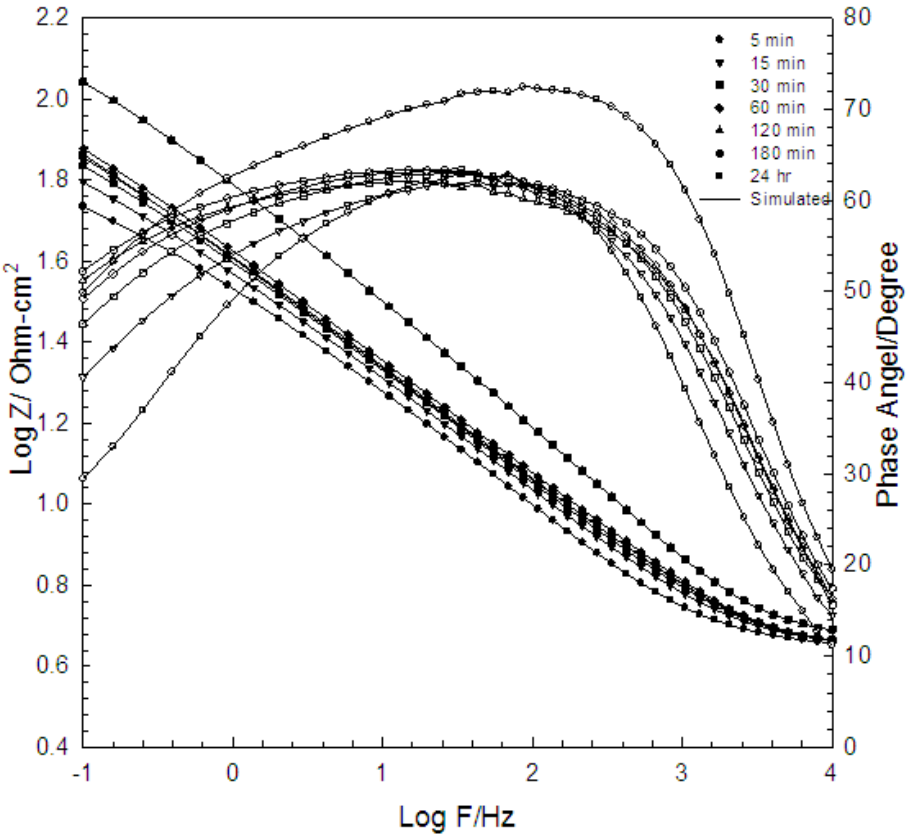

Fig. 6 (b): Bode plots of Cu-Al-Ni as a function of immersion time at 37^{o}C in SBF +Albumin

https://dx.doi.org/10.22161/ijaers/3.11.29 ISSN: 2349-6495(P) | 2456-1908(O)

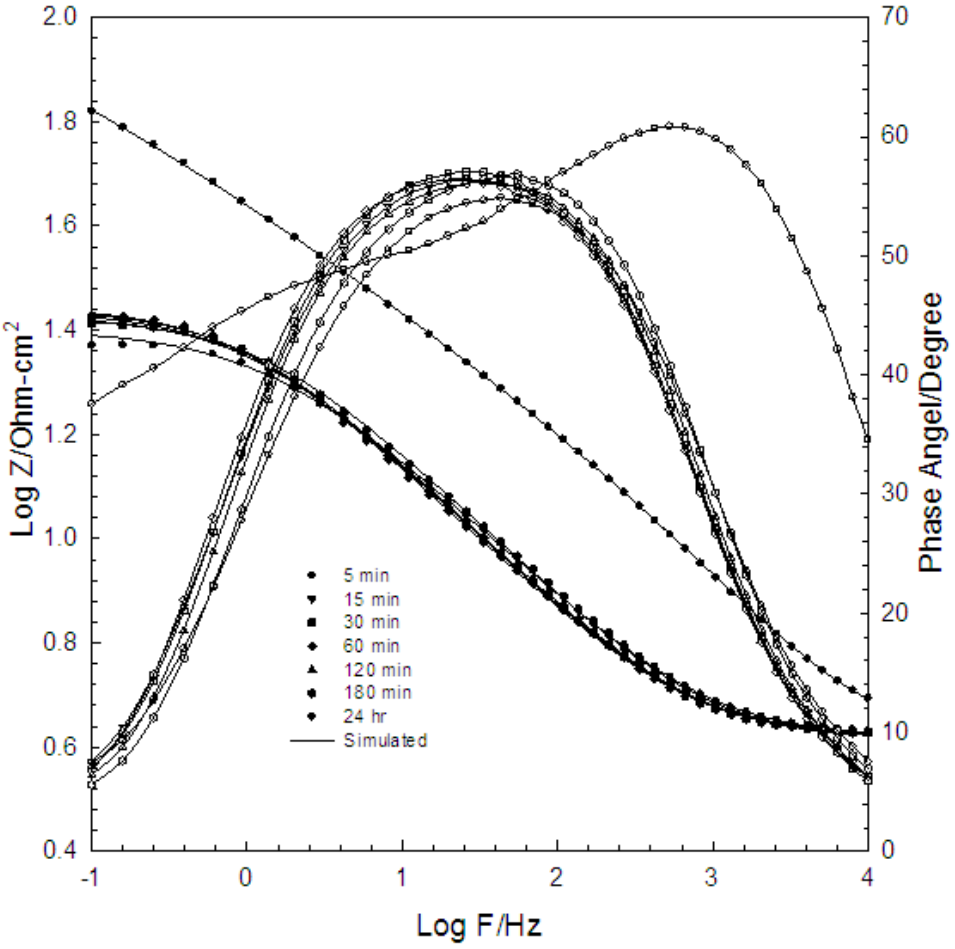

Fig. 6 c Bode plots of Cu-Al-Ni as a function of immersion time at 37^{o}C in SBF +KF

Fig. 7

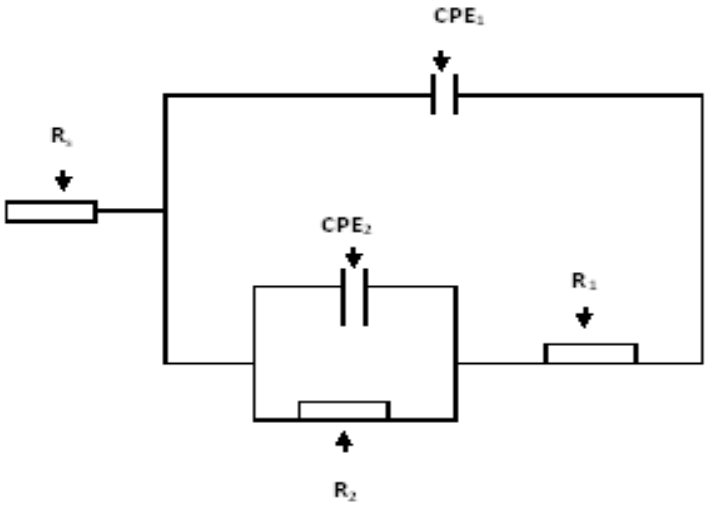

Fig. 7: The equivalent circuit

https://dx.doi.org/10.22161/ijaers/3.11.29 ISSN: 2349-6495(P) | 2456-1908(O)

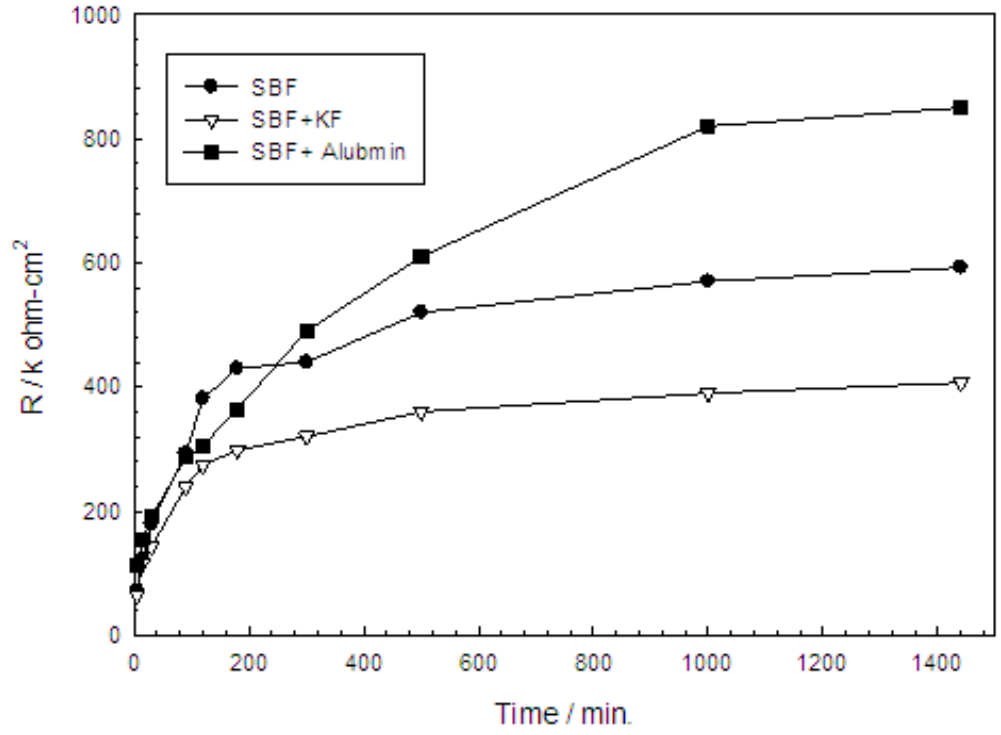

Fig. 8 (a): Change of the impedance with immersion time for Ti in different simulated body fluids

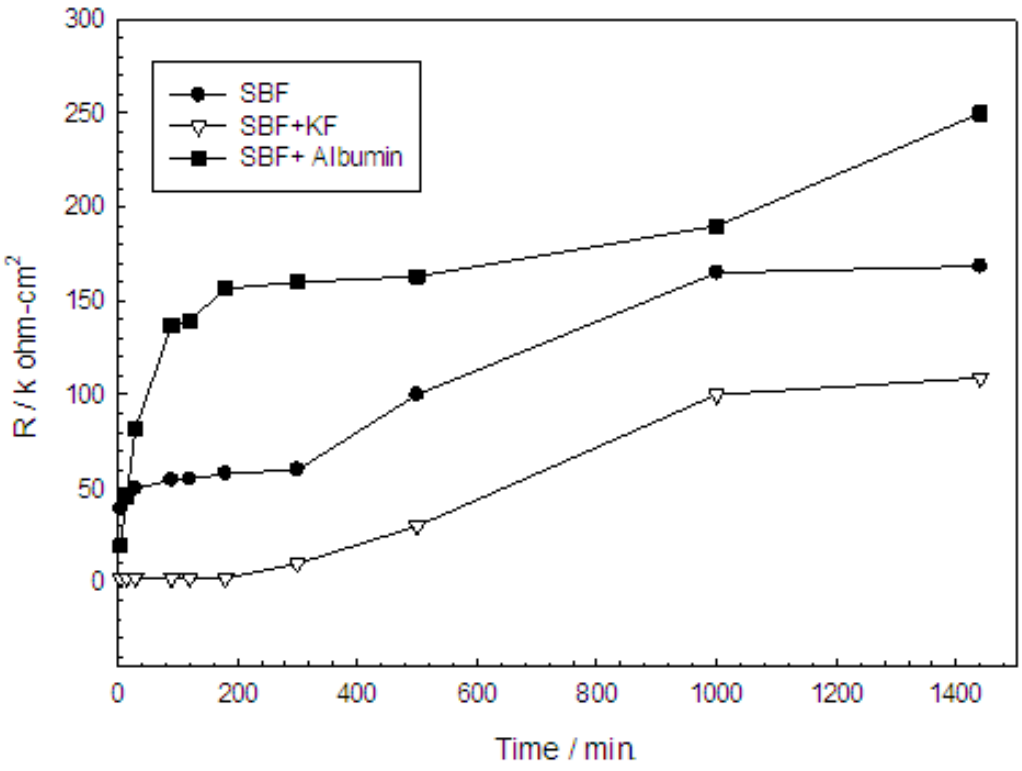

Fig. 8 (b): Change of the impedance with immersion time for Cu-Al-Ni in different simulated body fluids

https://dx.doi.org/10.22161/ijaers/3.11.29 *ISSN: 2349-6495(P) | 2456-1908(O)*

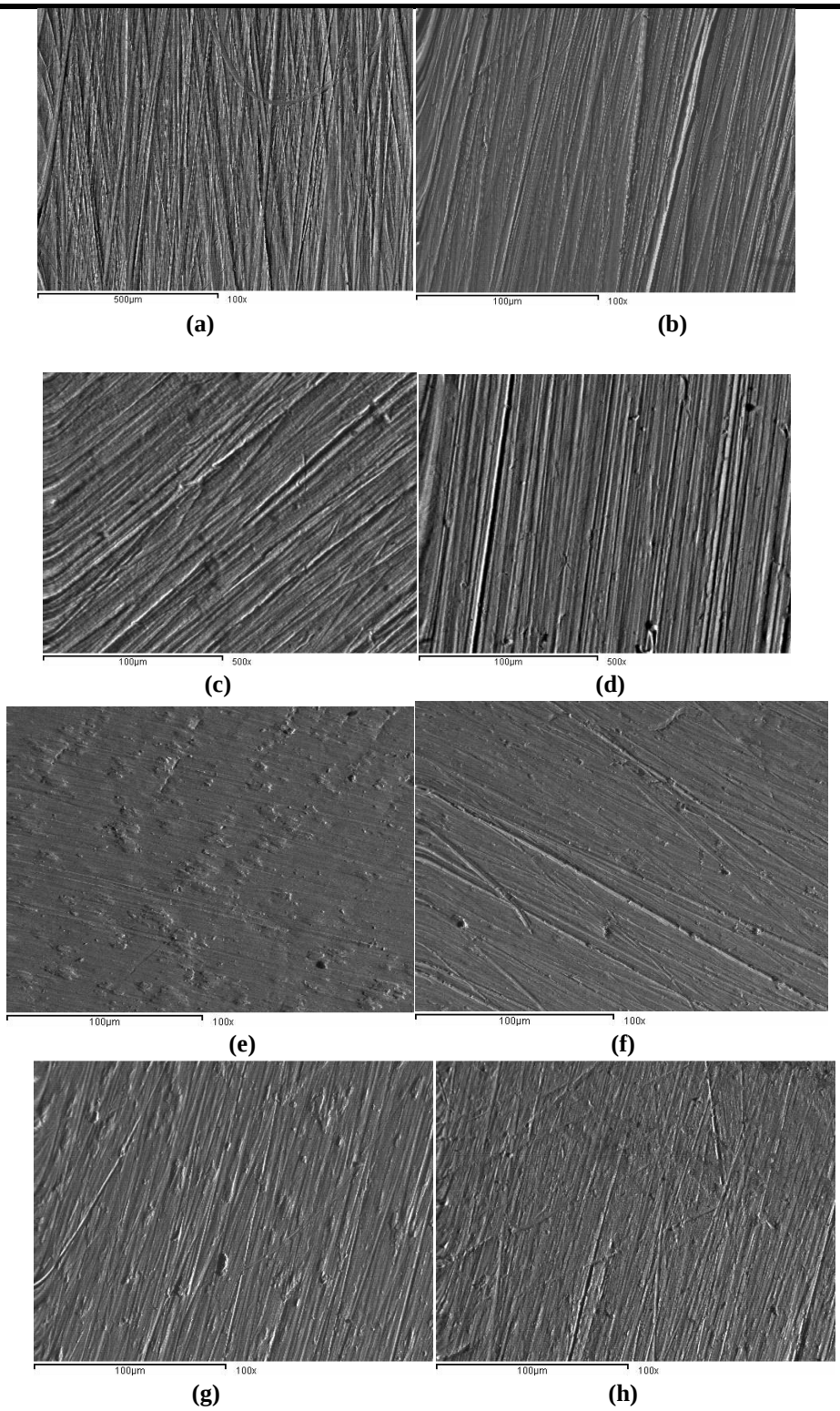

Fig. 9: Scanning electron microscopic images of samples after potentiodynamic testing; a) Polished Cu-Ni-Al, b) Cu-Al-Ni in SBF, c) Cu-Al-Ni in SBF + KF, d) Cu-Al-Ni in SBF + Albumin, e) Polished Ti, f) Ti in SBF, g) Ti in SBF +KF, h) Ti in SBF + Albumin.

https://dx.doi.org/10.22161/ijaers/3.11.29 *ISSN: 2349-6495(P) | 2456-1908(O)*

Table.1: Potentiodynamic corrosion data of Ti in SBF, SBF+KF and SBF+ Albumin solutions.

Medium	E_{corr} (mV)	i_{corr} (μA cm^{-2})	Ba (mV$decade^{-1}$)	Bc (mV$decade^{-1}$)
SBF	**-487.9**	**3.2**	**542**	**-626**
SBF+KF	**-563.4**	**5.0**	**617**	**-554**
SBF+Albumin	**-466.8**	**1.8**	**1220**	**-525**

Table.2: Potentiodynamic corrosion data of Cu-Al-Ni in SBF, SBF+KF and SBF+ Albumin solutions

Medium	E_{corr} (mV)	i_{corr} (μA cm^{-2})	Ba (mV$decade^{-1}$)	Bc (mV$decade^{-1}$)
SBF	-454	0.22	124	-754
SBF+ KF	-653	6.22	605	-511
SBF+Albumin	-425	0.062	86.5	-523

Table.3: Impedance parameters of Ti in SBF

Time/min.	R_s/ Ω	CPE_1/μF cm^{-2}	α_1	R_1/kΩ cm^2	CPE_2/μF cm^{-2}	α_2	R_2/kΩ cm^2
5	59.0	5.025	0.79	0.015	2.30	0.91	71.84
15	58.7	4.74	0.79	0.015	2.24	0.94	122.1
30	58.5	4.55	0.79	0.015	2.11	0.95	179.4
90	58.3	4.37	0.78	0.016	2.04	0.97	292.9
120	57.8	4.22	0.81	0.018	1.96	0.98	380.8
180	55.7	4.37	0.86	0.021	1.77	0.99	429.6
24 hr.	64.0	3.45	0.86	0.022	1.29	0.93	592.2

Table.4: Impedance parameters of Ti in SBF + KF

Time/min.	R_s/ Ω	CPE_1/μF cm^{-2}	α_1	R_1/kΩ cm^2	CPE_2/μF cm^{-2}	α_2	R_2/kΩ cm^2
5	45.5	3.5	0.71	0.061	0.42	0.99	65.2
15	64.5	10.2	0.82	0.075	1.78	0.99	116.2
30	64.9	10.0	0.83	0.076	1.77	0.99	142.8
90	64.5	9.75	0.84	0.075	1.76	0.99	238.7
120	65.1	9.72	0.84	0.075	1.76	0.99	274.8
180	68.0	9.50	0.85	0.077	1.75	0.99	297.5
24 hr.	74.0	8.60	0.87	0.088	1.62	0.99	406.8

Table.5: Impedance parameters of Ti in SBF + Albumin

Time/min.	R_s/ Ω	CPE_1/μF cm^{-2}	α_1	R_1/kΩ cm^2	CPE_2/μF cm^{-2}	α_2	R_2/kΩ cm^2
5	**59.7**	**4.175**	**0.81**	**0.0036**	**8.75**	**0.86**	**112.5**
15	**59.8**	**3.75**	**0.78**	**0.0064**	**8.50**	**0.92**	**154.8**
30	**64.1**	**3.95**	**0.78**	**0.0068**	**8.43**	**0.93**	**190.5**
90	**74.5**	**3.85**	**0.80**	**0.0064**	**8.08**	**0.93**	**286.7**
120	**70.8**	**3.87**	**0.81**	**0.0060**	**7.97**	**0.94**	**305.4**
180	**50.5**	**3.97**	**0.83**	**0.0048**	**7.67**	**0.92**	**364.0**
24 hr.	**52.5**	**4.20**	**0.93**	**0.0036**	**7.60**	**0.92**	**850.0**

https://dx.doi.org/10.22161/ijaers/3.11.29 *ISSN: 2349-6495(P) | 2456-1908(O)*

Table.6: Impedance parameters of Cu-Al-Ni in SBF

Time/min.	R_s/ Ω	CPE_1/μF cm^{-2}	α_1	R_1/kΩ cm^2	CPE_2/μF cm^{-2}	α_2	R_2/kΩ cm^2
5	*38.3*	*3.04*	*0.66*	*0.017*	*2.46*	*0.98*	*39.1*
15	*38.1*	*2.50*	*0.65*	*0.017*	*1.57*	*0.95*	*45.0*
30	*37.6*	*2.32*	*0.66*	*0.017*	*1.34*	*0.92*	*50.0*
90	*37.2*	*2.18*	*0.67*	*0.016*	*1.12*	*0.92*	*54.5*
120	*37.7*	*2.25*	*0.67*	*0.015*	*1.14*	*0.90*	*55.0*
180	*37.1*	*2.14*	*0.68*	*0.014*	*1.06*	*0.92*	*58.0*
24 hr.	*37.1*	*2.12*	*0.68*	*0.014*	*1.04*	*0.95*	*168.5*

Table.7: Impedance parameters of Cu-Al-Ni in SBF+ Albumin

Time/min.	R_s/ Ω	CPE_1/μF cm^{-2}	α_1	R_1/kΩ cm^2	CPE_2/μF cm^{-2}	α_2	R_2/kΩ cm^2
5	**35.6**	**2.07**	**0.63**	**0.0125**	**3.50**	**0.96**	**19.5**
15	**36.1**	**2.13**	**0.63**	**0.0120**	**3.68**	**0.93**	**46.1**
30	**36.3**	**2.10**	**0.65**	**0.0115**	**3.70**	**0.92**	**82.3**
90	**37.5**	**2.04**	**0.68**	**0.0105**	**3.58**	**0.87**	**136.8**
120	**38.1**	**2.04**	**0.68**	**0.0095**	**3.54**	**0.86**	**139.5**
180	**39.5**	**2.07**	**0.69**	**0.0065**	**2.40**	**0.83**	**156.6**
24 hr	**40.7**	**2.12**	**0.70**	**0.0050**	**3.53**	**0.83**	**250.0**

Table 8: Impedance parameters of Cu-Al-Ni in SBF + KF

Time/min.	R_s/ Ω	CPE_1/μF cm^{-2}	α_1	R_1/kΩ cm^2	CPE_2/μF cm^{-2}	α_2	R_2/kΩ cm^2
5	32.3	2.13	0.61	0.0045	7.46	0.77	1.97
15	32.7	2.28	0.65	0.0040	8.94	0.77	2.44
30	33.4	2.28	0.67	0.0035	9.24	0.77	2.45
90	33.7	2.19	0.69	0.0030	9.00	0.76	2.20
120	33.6	2.15	0.69	0.0025	8.80	0.76	2.30
180	34.1	1.99	0.65	0.0025	7.80	0.78	2.25
24 hr	36.9	0.594	0.55	0.0030	0.864	0.93	109.0